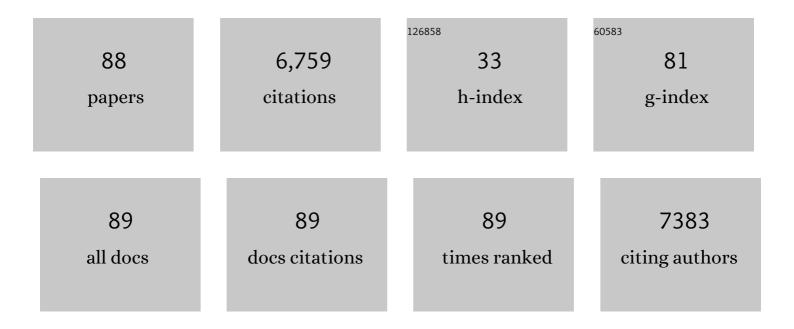
List of Publications by Year in descending order

Source: https://exaly.com/author-pdf/6140473/publications.pdf Version: 2024-02-01



TEDILLISA OHNO

#	Article	IF	CITATIONS
1	Preparation of S-doped TiO2 photocatalysts and their photocatalytic activities under visible light. Applied Catalysis A: General, 2004, 265, 115-121.	2.2	1,177
2	Photocatalytic Activity of S-doped TiO2Photocatalyst under Visible Light. Chemistry Letters, 2003, 32, 364-365.	0.7	860
3	Crystal faces of rutile and anatase TiO2 particles and their roles in photocatalytic reactions. New Journal of Chemistry, 2002, 26, 1167-1170.	1.4	724
4	Atomically dispersed antimony on carbon nitride for the artificial photosynthesis of hydrogen peroxide. Nature Catalysis, 2021, 4, 374-384.	16.1	474
5	Photoelectrochemical CO2 reduction by a p-type boron-doped g-C3N4 electrode under visible light. Applied Catalysis B: Environmental, 2016, 192, 193-198.	10.8	292
6	Shape-Controlled Anatase Titanium(IV) Oxide Particles Prepared by Hydrothermal Treatment of Peroxo Titanic Acid in the Presence of Polyvinyl Alcohol. Journal of Physical Chemistry C, 2009, 113, 3062-3069.	1.5	280
7	Trapping-Induced Enhancement of Photocatalytic Activity on Brookite TiO ₂ Powders: Comparison with Anatase and Rutile TiO ₂ Powders. ACS Catalysis, 2017, 7, 2644-2651.	5.5	191
8	Switching redox site of photocatalytic reaction on titanium(IV) oxide particles modified with transition-metal ion controlled by irradiation wavelength. Applied Catalysis A: General, 2008, 348, 148-152.	2.2	159
9	Photocatalytic Activity of a TiO2 Photocatalyst Doped with C4+ and S4+ Ions Having a Rutile Phase Under Visible Light. Catalysis Letters, 2004, 98, 255-258.	1.4	151
10	Degradation of Methylene Blue on Carbonate Species-doped TiO2Photocatalysts under Visible Light. Chemistry Letters, 2004, 33, 750-751.	0.7	150
11	Complete oxidation of acetaldehyde over a composite photocatalyst of graphitic carbon nitride and tungsten(VI) oxide under visible-light irradiation. Applied Catalysis B: Environmental, 2014, 150-151, 479-485.	10.8	106
12	Development of highly efficient sulfur-doped TiO2 photocatalysts hybridized with graphitic carbon nitride. Applied Catalysis B: Environmental, 2013, 142-143, 362-367.	10.8	101
13	Morphology control and characterization of broom-like porous CeO2. Chemical Engineering Journal, 2015, 260, 126-132.	6.6	91
14	Formation of new crystal faces on TiO2 particles by treatment with aqueous HF solution or hot sulfuric acid. New Journal of Chemistry, 2003, 27, 1304.	1.4	88
15	Synthesis of Y-doped CeO2/PCN nanocomposited photocatalyst with promoted photoredox performance. Applied Catalysis B: Environmental, 2019, 243, 513-521.	10.8	88
16	Photocatalytic reduction of CO2 over exposed-crystal-face-controlled TiO2 nanorod having a brookite phase with co-catalyst loading. Applied Catalysis B: Environmental, 2014, 152-153, 309-316.	10.8	83
17	Exposed crystal surface-controlled rutile TiO2 nanorods prepared by hydrothermal treatment in the presence of poly(vinyl pyrrolidone). Applied Catalysis B: Environmental, 2009, 91, 634-639.	10.8	75
18	Synthesis high specific surface area nanotube g-C ₃ N ₄ with two-step condensation treatment of melamine to enhance photocatalysis properties. RSC Advances, 2015, 5, 4026-4029.	1.7	75

#	Article	IF	CITATIONS
19	Photoexcited single metal atom catalysts for heterogeneous photocatalytic H2O2 production: Pragmatic guidelines for predicting charge separation. Applied Catalysis B: Environmental, 2021, 282, 119589.	10.8	74
20	Bandgap engineering of polymetric carbon nitride copolymerized by 2,5,8-triamino-tri-s-triazine (melem) and barbituric acid for efficient nonsacrificial photocatalytic H2O2 production. Applied Catalysis B: Environmental, 2020, 271, 118917.	10.8	72
21	Dependence of Photocatalytic Activity on Aspect Ratio of Shape-Controlled Rutile Titanium(IV) Oxide Nanorods. Journal of Physical Chemistry C, 2011, 115, 419-424.	1.5	59
22	Dependence of Activity of Rutile Titanium(IV) Oxide Powder for Photocatalytic Overall Water Splitting on Structural Properties. Journal of Physical Chemistry C, 2014, 118, 9093-9100.	1.5	59
23	(Au@Ag)@Au double shell nanoparticles loaded on rutile TiO2 for photocatalytic decomposition of 2-propanol under visible light irradiation. Applied Catalysis B: Environmental, 2016, 180, 255-262.	10.8	59
24	Synthesis and photocatalytic performance of yttrium-doped CeO2 with a porous broom-like hierarchical structure. Applied Catalysis B: Environmental, 2016, 183, 361-370.	10.8	57
25	Cu2O/TiO2 decorated on cellulose nanofiber/reduced graphene hydrogel for enhanced photocatalytic activity and its antibacterial applications. Chemosphere, 2022, 286, 131731.	4.2	57
26	Improving g-C 3 N 4 photocatalytic performance by hybridizing with Bi 2 O 2 CO 3 nanosheets. Catalysis Today, 2017, 284, 27-36.	2.2	54
27	Design and Synthesis of Sm, Y, La and Ndâ€doped CeO ₂ with a broomâ€like hierarchical structure: a photocatalyst with enhanced oxidation performance. ChemCatChem, 2020, 12, 2638-2646.	1.8	51
28	Boosting visible-light-driven photocatalytic performance of waxberry-like CeO2 by samarium doping and silver QDs anchoring. Applied Catalysis B: Environmental, 2021, 286, 119845.	10.8	51
29	Improvement of photocatalytic activity of brookite titanium dioxide nanorods by surface modification using chemical etching. Applied Surface Science, 2012, 258, 5803-5809.	3.1	47
30	Photoelectrochemical Homocoupling of Methane under Blue Light Irradiation. ACS Energy Letters, 2019, 4, 502-507.	8.8	46
31	Effect of core@shell (Au@Ag) nanostructure on surface plasmon-induced photocatalytic activity under visible light irradiation. Applied Catalysis B: Environmental, 2017, 211, 11-17.	10.8	45
32	Porous cerium dioxide hollow spheres and their photocatalytic performance. RSC Advances, 2014, 4, 62255-62261.	1.7	39
33	Development of the Visibleâ€Light Response of CeO _{2â^'<i>x</i>} with a high Ce ³⁺ Content and Its Photocatalytic Properties. ChemCatChem, 2018, 10, 1267-1271.	1.8	37
34	A new precursor to synthesize g-C ₃ N ₄ with superior visible light absorption for photocatalytic application. Catalysis Science and Technology, 2017, 7, 1826-1830.	2.1	35
35	Photooxidation of organic compounds in a solution containing hydrogen peroxide and TiO2 particles under visible light. Journal of Applied Electrochemistry, 2005, 35, 793-797.	1.5	33
36	Dependence of photocatalytic activity on aspect ratio of a brookite TiO2 nanorod and drastic improvement in visible light responsibility of a brookite TiO2 nanorod by site-selective modification of Fe3+ on exposed faces. Journal of Molecular Catalysis A, 2015, 396, 261-267.	4.8	31

#	Article	IF	CITATIONS
37	Photocatalytic Hydrogen or Oxygen Evolution from Water over S- or N-Doped TiO2under Visible Light. International Journal of Photoenergy, 2008, 2008, 1-7.	1.4	30
38	Platinum and indium sulfide-modified Cu ₃ BiS ₃ photocathode for photoelectrochemical hydrogen evolution. Journal of Materials Chemistry A, 2017, 5, 10450-10456.	5.2	30
39	Visible-light-driven photocatalytic disinfection of raw surface waters (300–5000 CFU/mL) using reusable coated Ru/WO3/ZrO2. Journal of Hazardous Materials, 2021, 402, 123514.	6.5	29
40	Oxygen induced enhancement of NIR emission in brookite TiO ₂ powders: comparison with rutile and anatase TiO ₂ powders. Physical Chemistry Chemical Physics, 2018, 20, 3241-3248.	1.3	28
41	Improvement of photocatalytic activity of high specific surface area graphitic carbon nitride by loading a co-catalyst. Rare Metals, 2019, 38, 468-474.	3.6	28
42	Titanium Dioxide/Polyvinyl Alcohol/Cork Nanocomposite: A Floating Photocatalyst for the Degradation of Methylene Blue under Irradiation of a Visible Light Source. ACS Omega, 2021, 6, 14493-14503.	1.6	28
43	Novel cerium-based MOFs photocatalyst for photocarrier collaborative performance under visible light. Journal of Catalysis, 2022, 405, 74-83.	3.1	27
44	Visible light-driven H2O2 synthesis by a Cu3BiS3 photocathode via a photoelectrochemical indirect two-electron oxygen reduction reaction. Applied Catalysis B: Environmental, 2022, 307, 121152.	10.8	25
45	Improvement of selectivity for CO ₂ reduction by using Cu ₂ ZnSnS ₄ electrodes modified with different buffer layers (CdS and) Tj ETQq1 1 0	784 1.1 ⁄4 rgBT	¯ Øverlock 1
46	Development of visible-light-responsive morphology-controlled brookite TiO2 nanorods by site-selective loading of AuAg bimetallic nanoparticles. Applied Catalysis B: Environmental, 2019, 245, 681-690.	10.8	24
47	Synthesis of anatase TiO2 with exposed {001} and {101} facets and photocatalytic activity. Rare Metals, 2019, 38, 287-291.	3.6	24
48	Infrared response in photocatalytic polymeric carbon nitride for water splitting via an upconversion mechanism. Communications Materials, 2020, 1, .	2.9	23
49	Cascade use of bamboo as raw material for several high value products: production of xylo-oligosaccharide and activated carbon for EDLC electrode from bamboo. Journal of Porous Materials, 2018, 25, 1541-1549.	1.3	20
50	New approach for synthesis of activated carbon from bamboo. Journal of Porous Materials, 2016, 23, 349-355.	1.3	19
51	Solar-driven H2 evolution over CuNb2O6: Effect of two polymorphs (monoclinic and orthorhombic) on optical property and photocatalytic activity. Journal of Photochemistry and Photobiology A: Chemistry, 2018, 356, 263-271.	2.0	19
52	Improvement of Thermoelectric Performance for Sb-Doped SnO2 Ceramics Material by Addition of Cu as Sintering Additive. Journal of Electronic Materials, 2014, 43, 3567-3573.	1.0	18
53	Control of the crystal structure of titanium(IV) oxide by hydrothermal treatment of a titanate nanotube under acidic conditions. CrystEngComm, 2010, 12, 532-537.	1.3	17
54	Photoelectrochemical water vapor splitting using an ionomer-coated rutile TiO ₂ thin layer on titanium microfiber felt as an oxygen-evolving photoanode. Sustainable Energy and Fuels, 2019, 3, 2048-2055.	2.5	17

#	Article	IF	CITATIONS
55	The role of Ce addition in catalytic activity enhancement of TiO ₂ -supported Ni for CO ₂ methanation reaction. RSC Advances, 2020, 10, 26952-26971.	1.7	17
56	Hydrothermally Reduced Graphene Hydrogel Intercalated with Divalent Ions for Dye Adsorption Studies. Processes, 2021, 9, 169.	1.3	17
57	Preparation of luminescent polystyrene microspheres via surface-modified route with rare earth (Eu3+ and Tb3+) complexes linked to 2,2′-bipyridine. Rare Metals, 2015, 34, 590-594.	3.6	16
58	Development of Plasmonic Photocatalyst by Siteâ€selective Loading of Bimetallic Nanoparticles of Au and Ag on Titanium(IV) Oxide. ChemCatChem, 2020, 12, 3783-3792.	1.8	16
59	Accessing effects of aliphatic dicarboxylic acid towards the physical and chemical changes in low temperature hydrothermally reduced graphene hydrogel. Journal of Porous Materials, 2021, 28, 1291-1300.	1.3	16
60	Fabrication of a porous ZnRh ₂ O ₄ photocathode for photoelectrochemical water splitting under visible light irradiation and a significant effect of surface modification by ZnO necking treatment. Journal of Materials Chemistry A, 2016, 4, 6116-6123.	5.2	13
61	Selective oxidation of benzaldehyde derivatives on TiO2 photocatalysts modified with fluorocarbon group. Catalysis Letters, 2005, 102, 207-210.	1.4	12
62	Catalytic Graphitization for Preparation of Porous Carbon Material Derived from Bamboo Precursor and Performance as Electrode of Electrical Double-Layer Capacitor. Journal of Electronic Materials, 2015, 44, 4933-4939.	1.0	12
63	Initial step of anthracene-sensitized photoacid generation from diphenyliodonium hexafluorophosphate in an epoxy matrix studied by steady-state and laser-flash photolyses. Journal of Polymer Science, Part B: Polymer Physics, 2001, 39, 2937-2946.	2.4	11
64	Photochemistry and photocuring properties of thiol-substituted α-aminoalkylphenone as radical photoinitiator. Journal of Polymer Science, Part B: Polymer Physics, 2005, 43, 1684-1695.	2.4	11
65	Development of Visible Light Sensitive TiO ₂ Photocatalysts and Their Sensitization Using Fe ³⁺ lons. Journal of the Japan Petroleum Institute, 2006, 49, 168-176.	0.4	11
66	Fabrication of morphology-controlled TiO2 photocatalyst nanoparticles and improvement of photocatalytic activities by modification of Fe compounds. Rare Metals, 2015, 34, 291-300.	3.6	11
67	Photoelectrochemical synthesis of aniline from nitrobenzene in a neutral aqueous solution by using a p-type Cu2ZnSnS4 electrode. Applied Catalysis B: Environmental, 2018, 225, 445-451.	10.8	11
68	Recent Progress in Photocatalytic Efficiency of Hybrid Three-Dimensional (3D) Graphene Architectures for Pollution Remediation. Topics in Catalysis, 2022, 65, 1634-1647.	1.3	11
69	Effects of the Atmosphere in a Hydrothermal Process on the Morphology and Photocatalytic Activity of Cerium Oxide. ChemCatChem, 2018, 10, 4269-4273.	1.8	9
70	Nitrogen and sulfur co-doped CeO ₂ nanorods for efficient photocatalytic VOCs degradation. Catalysis Science and Technology, 2022, 12, 5203-5209.	2.1	9
71	Photocatalytic partial oxidation of methylpyridine isomers on TiO2 particles under an anaerobic condition. Journal of Applied Electrochemistry, 2005, 35, 783-791.	1.5	7
72	Spherical activated carbon derived from spherical cellulose and its performance as EDLC electrode. Journal of Applied Polymer Science, 2014, 131, .	1.3	7

#	Article	IF	CITATIONS
73	Preparation of Porous Carbon Material Derived from Cellulose with Added Melamine Sulfate and Electrochemical Performance as EDLC Electrode. Journal of Electronic Materials, 2019, 48, 879-886.	1.0	7
74	KOH activation of solid residue of Japanese citron after extraction by microwave process and property as EDLC electrode. Journal of Porous Materials, 2020, 27, 727-734.	1.3	7
75	Performance as electrode of electrical double layer capacitor of activated carbon prepared from bamboo using guanidine phosphate and CO2 activation. Journal of Porous Materials, 2017, 24, 1507-1512.	1.3	6
76	Visible-Light-Induced Hydrophilic Conversion of an S-Doped TiO2 Thin Film and Its Photocatalytic Activity for Decomposition of Acetaldehyde in Gas Phase. Journal of the Ceramic Society of Japan, 2007, 115, 310-314.	1.3	4
77	Photo-sensitive 2D Arrangement of â^'OH/H ₂ O on Brookite TiO ₂ (210). Journal of Physical Chemistry C, 2020, 124, 19091-19100.	1.5	4
78	Inclusion of fullerene in polymer chains grafted on silica nanoparticles in an organic solvent. Polymer Journal, 2014, 46, 623-627.	1.3	3
79	Functionalized Graphitic Carbon Nitrides for Photocatalytic H ₂ 0 ₂ Production: Desired Properties Leading to Rational Catalyst Design. KONA Powder and Particle Journal, 2023, 40, 124-148.	0.9	2
80	Synthesis of diamond film and UNCD on BeCu substrate by hot filament CVD. Journal of the Ceramic Society of Japan, 2013, 121, 187-194.	0.5	1
81	Colloidal crystallization of C60/polymer-grafted silica particles in organic solvent. Colloid and Polymer Science, 2015, 293, 2075-2081.	1.0	1
82	Photocatalytic Synthesis of <i>p</i> â€Anisaldehyde in a Mini Slurryâ€Bubble Reactor under Solar Light Irradiation. Canadian Journal of Chemical Engineering, 2020, 98, 119-126.	0.9	1
83	New Method for the Synthesis of a Photocatalyst by Using Intercalation of Amines in K2Ti4O9. Journal of Advanced Oxidation Technologies, 2007, 10, .	0.5	0
84	CVD Synthesis of single-walled carbon nanotubes from CH4 gas by using zeolite. Tanso, 2007, 2007, 310-315.	0.1	0
85	Synthesis of carbon nanotube in organic liquids carbon source on La2NiO4 ceramics catalyst. Journal of the Ceramic Society of Japan, 2008, 116, 284-287.	0.5	0
86	Facile preparation and characterization of luminescent polystyrene composite microspheres. New Journal of Chemistry, 2013, 37, 2133.	1.4	0
87	Synthesis of carbon/limonite composite through CVD method. Tanso, 2007, 2007, 324-328.	0.1	0
88	A homogeneous copper bismuth sulfide photocathode prepared by spray pyrolysis deposition for efficient photoelectrochemical hydrogen generation. Materials Letters, 2022, 325, 132801.	1.3	0